Model for the Kinematics of Polymer Dissolution

Abstract: The dissolution of glassy polymers is described by a phenomenological model of the motion of two boundaries: the liquid-gel boundary and the gel-glass boundary. The motion of these boundaries, as well as the concentration profile in the layers of a dissolving polymer, was obtained by numerical solution of the Stefan boundary value problem. Confirmation of the experimental program written to simulate the problem is established by its good agreement with direct observation of the dissolution dynamics of polystyrene in methyl ethyl ketone. A potential application of this model to the study of the dissolution dynamics of other polymer-solvent systems is done by simulating the dissolution of three types of polymer-solvent pairs: 1) swelling of rubber, 2) high glass transition concentration, and 3) low glass transition concentration. Contrasting dissolution characteristics are shown for the effect of different types of polymer-solvent pairs as well as for the effect of different molecular weights for the same type of polymer-solvent pair.

Introduction

The polymer dissolution phenomenon has been of interest to the scientific community for at least three decades. However, industrial interest in this subject has only recently been aroused by the advent of the large scale integrated circuit, where the preferred fabrication method is the lithographic technique. In particular, the use of polymers as electron beam resist materials has intensified this interest.

It was observed [1] that when a region of a film of poly(methyl methacrylate), PMMA, is exposed to an electron beam, it dissolves many times faster than do unexposed areas. By careful choice of solvents (developers), an image can be developed in the polymer surface, with geometrical integrity, of lines narrower than 1 μ m spaced less than 1 μ m apart. The direction of this technology is toward narrower lines and greater line density. Therefore, it is important that the geometric integrity of the radiation exposure pattern be maintained during the development process, and this requires a greater and deeper understanding of the nature of polymer dissolution.

In response to this need, we initiated a study of the kinematics of polymer dissolution. The first step was a formulation of a mathematical model which describes, phenomenologically, the Fickian diffusions involved in the development process. The model takes into account the effect upon the contrast and resolution of the developed image of the resist due to the different material parameters (transport and thermodynamic properties) as well as the processing parameters (geometry and stirring speeds, etc.).

To verify the model and the computer simulation of the polymer dissolution, experimental techniques for the direct observation of the dissolution process were developed concurrently. Polystyrene dissolving in methyl ethyl ketone (MEK) was the system used for the experimental verification of the model, because many of the material parameters required for the computer simulation are readily available in the open literature. For example, the diffusion coefficients of MEK in polystyrene have already been obtained by Ueberreiter [2] and the other material parameters have been published by Berry and Fox [3] and by Graessley [4]. Using the model we have investigated the effect of several parameters on the kinematics of the swelling and dissolution processes. These parameters include the diffusion coefficients of the solvent in the polymer matrix and of the polymer in the solvent, and the polymer molecular weight.

Physical concept of the model

In a dissolving polymer, two distinct boundaries or interfaces characterized by a sharp change in the concentration of the solvent may exist. These boundaries can be observed because of sharp changes in the refractive index, viscosity, and modulus at the interfaces. These viscosity and modulus changes are useful because they allow the mechanical properties of the different phases between these boundaries to be characterized.

The first boundary, between the liquid and the gel-like solution phases, is particularly significant, for it is here that the partition between the dissolved and the undissolved polymer is likely to occur should the polymer be

taken out of contact with the solvent. For a given polymer-solvent pair and polymer molecular weight, the concentration at the liquid-gel boundary is a defined quantity. For example, the product of the polymer molecular weight and the concentration $(c_{\rm F})$ at the liquid-gel interface of polystyrene dissolving in MEK at room temperature has been reported to be approximately 27000 [3, 4].

At the liquid-gel interface, it is envisioned that the polymer molecules go from the gel-like phase (entangled state) to the less viscous liquid solution (free state) at a rate which is defined as the disassociation rate (R). Of all the material parameters required in this model, the most difficult to define from an analytic point of view is this disassociation rate. Intuitively, it is reasonable to relate R to the osmotic pressure as the driving force, and to the segmental stiffness (chain friction coefficient) as the resisting force. Thus, R must be related to the viscosity phenomena of highly concentrated polymer solutions. However, the complexity of this relaxation process prevents a quantitative prediction of R from the molecular properties of the polymer and the solvent. Experimentally, R may be estimated by extrapolating the solubility rate to very high solvent velocity across the liquid-gel interface. Our simulation results indicate that this method of estimating the value of R is valid because the solubility rate at this condition is controlled primarily by R, and it is no longer affected by the diffusion of the dissolved polymer across the boundary layer.

The second boundary lies between the gel-like and the glass-like phases. Again, this interface is characterized by a defined concentration. In addition to a sharp change in refractive index, this boundary is also marked by a steep change in the diffusion coefficient of the solvent in the polymer matrix. The highly nonlinear concentration dependence of the diffusion coefficient is well known [2] and, as will be shown, plays a major role in the dynamics of polymer dissolution. Once the concentrations at these boundaries are defined and the different material parameters (diffusion coefficients of the solvent and polymer and R) are known, the kinematics of dissolution can be formulated and the spatial locations of the liquid-gel and gel-glass interfaces tracked with time. Thus, the kinematics of the swelling and the dissolution of the polymer may be described analytically. We define the following physical parameters:

- Disassociation concentration $c_{\rm F}-$ the volume concentration of the polymer at the gel-liquid interface; $0 < c_{\rm F} < 1$.
- Disassociation rate R—the rate in cm/s at which the disassociated polymer molecules are freed to diffuse into the liquid solution from the gel-liquid interface.

- Glass-gel interface concentration $c_{\rm G}$ —the volume concentration of the polymer at which the diffusion coefficient of solvent begins a sharp decrease: $c_{\rm F} < c_{\rm G} < 1$.
- Nominal diffusion coefficient of solvent in polymer (D_s) – the diffusion coefficient of solvent in polymer at the gel-liquid interface in cm²/s.
- Nominal diffusion coefficient of polymer in liquid solution D_p-the diffusion coefficient of polymer in dilute solution in cm²/s.
- Gel-liquid interface y(t) position of the gel-liquid interface at time t in cm.
- Glass-gel interface $x_{\rm G}(t)$ position in the polymer where the volume concentration is $c_{\rm G}$ at time $t, y(t) < x_{\rm G}(t)$.
- Boundary layer thickness B—thickness in the liquid solution, measured from the gel-liquid interface to a point in the liquid phase where concentration of the polymer may be taken to be zero. The boundary layer is established by flow in the liquid phase due to mechanical stirring of the solvent.

The space coordinate x is directed into the polymer and x = 0 coincides with the gel-liquid interface at time t = 0. Thus, y(0) = 0; c_F and R are dependent upon the molecular weight of the polymer, but they are independent of each other in the model.

Mathematical formulation of the boundary value problem

In addition to the physical considerations discussed in the previous section, we assume that the conditions of constant disassociation concentration and constant disassociation rate are established immediately upon wetting of the polymer surface, and that the solvent and the polymer are incompressible. The following notations are introduced in addition to those defined previously:

- c Volume concentration of polymer, 0 < c < 1;
- c' Volume concentration of solvent, c' = 1 c;
- H_p Initial thickness of polymer film when $c \equiv 1$, i.e., polymer occupies the region $0 < x < H_p$ at t = 0;
- $f_{\rm s}(c)$ Numerical factor for the diffusion coefficient of solvent in polymer. Hence the local diffusion coefficient of solvent in polymer is equal to $D_{\rm s}f_{\rm s}(c)$. $f_{\rm s}(c)>0, f_{\rm s}(c_{\rm F})=1;$
- $f_{\rm p}(c)$ Numerical factor for the diffusion coefficient of dissolved polymer in liquid solution. Hence, the local diffusion coefficient of polymer in liquid solution is equal to $D_{\rm p}f_{\rm p}(c)$ and $f_{\rm p}(c)>0$, $f_{\rm p}(0)=1$;
- q(x, t) Local flux of dissolved polymer in liquid solution in cm/s;
- q'(x, t) Local flux of solvent in polymer in cm/s; and v(x, t) Swelling rate of polymer at x and time t in cm/s.

The local flux of solvent passing through any material point x in the polymer is given in terms of the concentration of solvent c' by

$$q'(x,t) = -D_{c}f_{c}(c) \ \partial c'/\partial x, \qquad x > y(t). \tag{1}$$

Similarly, the local flux of polymer in liquid solution is given by

$$q(x,t) = -D_{p}f_{p}(c)\frac{\partial c}{\partial x}, \quad x < y(t).$$
 (2)

• Swelling of the polymer

As solvent diffuses into the polymer, the latter swells at the rate v(x, t), equal in magnitude but opposite in direction to the flux q'(x, t) of the solvent at x and t; hence,

$$v(x, t) = -q'(x, t), \quad y(t) < x < H_{p}.$$

However, at the gel-liquid interface, x = y(t); the interface position is determined by the equation

$$dy/dt = v[x = y^{+}(t), t] - q[x = y^{-}(t), t], \tag{4}$$

where $q[x = y^-(t), t]$ is the flux of dissolved polymer leaving the interface, and $y^\pm(t)$ indicate the gel and the liquid solution sides of the interface y(t), respectively. The effect of swelling was investigated by Wang and Kwei [5] based on constant swelling rate, independent of x and t.

• Diffusion of solvent in the polymer, $y^+(t) < x < H_p$ Observed from a coordinate moving with the swelling rate v(x, t) of the polymer material at x, the local flux of solvent is q'. The absolute flux of solvent as seen by the stationary observer is, therefore, q' + c'v. Consequently, the conservation equation becomes

$$\frac{\partial c'}{\partial t} + \frac{\partial}{\partial x} \left(q' + c'v \right) = 0, \qquad y^+(t) < x < H_p. \tag{5}$$

Since c' = 1 - c, the conservation equation may be expressed in terms of c by means of Eqs. (1) and (3) in the form

$$\frac{\partial c}{\partial t} = D_{\rm s} \frac{\partial}{\partial x} \left[f_{\rm s}(c) \ c \frac{\partial c}{\partial x} \right], \qquad y^{+}(t) < x < H_{\rm p}. \tag{6}$$

Initially, $c' \equiv 0$; hence,

$$c(x, t = 0) \equiv 1, \quad y^{+}(0) = 0 < x < H_{p}.$$
 (7)

At the gel-liquid interface, $x = y^+(t)$, the concentration is kept at constant $c_{\rm F}$. For an impervious substrate at $x = H_{\rm p}$, the flux vanishes. Thus, the boundary conditions for c are

$$c = c_{\rm F}$$
 at $x = y^{+}(t)$, $t > 0$;
 $\frac{\partial c}{\partial x} = 0$ at $x = H_{\rm p}$, $t > 0$. (8)

At the glass-gel interface, both c and the flux $D_{\rm s}f_{\rm s}(c)$ $\partial c/\partial x$ must be continuous.

• Diffusion of dissolved polymer in the liquid solution, $x < y^{-}(t)$

The swelling of the polymer causes a bulk motion in the liquid phase (dilute solution) at the velocity of the gelliquid interface given by Eq. (4). Observed from a coordinate moving with the liquid solution at velocity dy/dt, the local flux of polymer in the solution is q. The absolute flux of polymer in solution (as seen from a stationary coordinate) is, therefore, q + c dy/dt. Hence, the conservation equation becomes

$$\frac{\partial c}{\partial t} + \frac{\partial}{\partial x} \left(q + c \, \frac{dy}{dt} \right) = 0, \qquad x < y^{-}(t). \tag{9}$$

Making use of Eq. (2), we derive the conservation equation in terms of c:

$$\frac{\partial c}{\partial t} + \frac{dy}{dt} \frac{\partial c}{\partial x} = D_{\mathfrak{p}} \frac{\partial}{\partial x} \left[f_{\mathfrak{p}}(c) \frac{\partial c}{\partial x} \right], \qquad x < y^{-}(t) . \tag{10}$$

Initially,

$$c(x, t = 0) \equiv 0, \quad x < y^{-}(0) = 0.$$
 (11)

At the gel-liquid interface, $x = y^{-}(t)$, the flux of dissolved polymer leaving the interface is computed according to

$$q[x = y^{-}(t), t] = -D_{p}f_{p}(c) \partial c/\partial x$$
 at $y = y^{-}(t),$
 $t \ge 0.$ (12)

Depending on the condition at the gel-liquid interface, either of the following may take place:

1. Starting from time t = 0, the flux given by Eq. (12) is limited by the disassociation rate R of the dissociated polymer molecules that are available from the gelliquid interface. Hence,

$$-q(x = y^{-}(t), t) = D_{p} f_{p}(c) \ \partial c / \partial x = R$$
at $x = y^{-}(t), \quad 0 < t < t_{c},$ (13)

for some t_c , provided $c < c_F$ at $x = y^-(t)$. Gradually, the concentration c at $x = y^-(t)$, which is zero at t = 0, increases as long as $0 < c < c_F$ at $x = y^-(t)$. During these times, the diffusion capability is always sufficient to carry away whatever dissolved polymer is available at the interface.

2. In the end, $c = c_F$ at $x = y^-(t)$ for $t > t_c$, because the diffusion capability becomes insufficient to carry away the dissolved polymer molecules that continue to be available at the disassociation rate R. Thereafter, the concentration c at $x = y^-(t)$ is maintained at c_F . Hence,

$$c = c_{\rm F}$$
 at $x = y^{-}(t)$, $t > t_{\rm c}$. (14)

At $t = t_c$, both Eqs. (13) and (14) are satisfied.

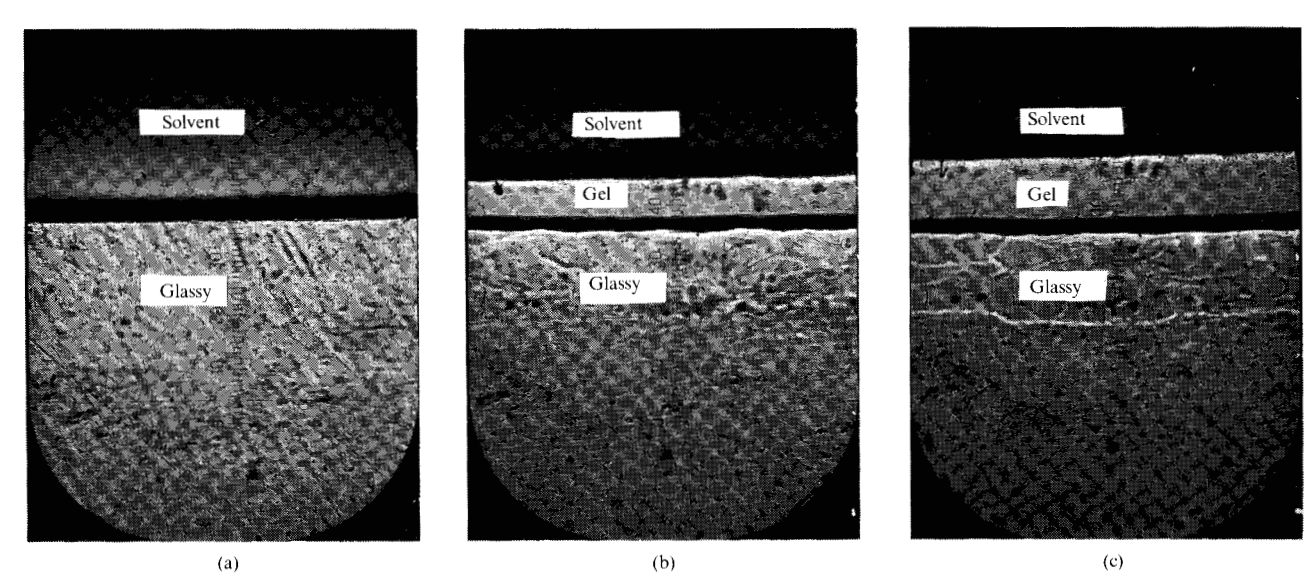


Figure 1 Photomicrographs of NBS-705 in contact with methyl ethyl ketone (MEK): (a) after a few seconds, (b) after 200 seconds, and (c) after about 1000 seconds.

When the condition (13) is valid, we call this "sourcelimited analysis." When the condition (14) prevails, we call this "flux-limited analysis." Phenomenologically, the dissolution process may be referred to as disassociationrate-controlled in the former case and as diffusion-controlled in the latter case.

The second boundary condition at the boundary layer is given by

$$c = 0$$
 at $x = y^{-}(t) - B$. (15)

Since $f_p(0) = 1$, the rate of removal of dissolved polymer may be computed according to

$$q_{B} = -D_{p} \partial c/\partial x, \qquad x = y^{-}(t) - B. \tag{16}$$

For the gel-liquid interface given by Eq. (4), the velocity may be expressed in terms of c by using (1), (2), and the condition $f_c(c_F) = 1$:

$$\frac{dy}{dt} = D_{p} f_{p}(c) \frac{\partial c}{\partial x} \Big|_{x=y^{-}(t)} - D_{s} \frac{\partial c}{\partial x} \Big|_{x=y^{+}(t)}.$$
(17)

Mathematical solution

By introducing the dimensionless time variable τ defined by

$$\tau = D_{c}t/H_{p}^{2},\tag{18}$$

and normalizing all linear dimensions with respect to the initial film thickness H_p , the boundary value problem defined in Eqs. (5) through (17) may be interpreted by means of the following dimensionless parameters:

$$y^*(\tau) = y(t)/H_p,$$
 $x_G^*(\tau) = x_G(t)/H_p,$
 $B^* = B/H_p,$
 $r^* = D_p/D_s,$
 $R^* = H_pR/D_p,$ and
 $x^* = x/H_p.$ (19)

• Diffusion of solvent in polymer, $y^{*+}(\tau) < x^* < 1$ The differential equation can be written as

$$\frac{\partial c}{\partial \tau} = \frac{\partial}{\partial x^*} \left[f_{\rm s}(c) c \, \frac{\partial c}{\partial x^*} \right],\tag{20}$$

with the initial condition

$$c(x^*, \tau = 0) = 1, \quad y^{*+}(0) = 0 < x^* < 1,$$
 (21)

and the boundary conditions

$$c = c_{\text{F}}, \quad x^* = y^{*+}(\tau), \quad \tau > 0;$$

 $\partial c / \partial x^* = 0, \quad x^* = 1, \quad \tau > 0.$ (22)

• Diffusion of dissolved polymer in the liquid, $y^{*-}(\tau) - B^* < x^* < y^{*-}(\tau)$

For the differential equation,

$$\frac{\partial c}{\partial \tau} = -\frac{dy^*}{d\tau} \frac{\partial c}{\partial x^*} + r^* \frac{\partial}{\partial x^*} \left[f_{p}(c) \frac{\partial c}{\partial x^*} \right]; \tag{23}$$

for the initial condition,

$$c(x^*, \tau = 0) \equiv 0, \quad -B^* < x^* < y^{*^-}(0) = 0;$$
 (24)

and for the boundary conditions,

$$c = 0, x^* = y^{*-}(\tau) - B^*.$$
 (25)

1. Source-limited analysis, if $0 < c < c_{\rm F}$ at $x^* = y^{*^-}(\tau)$, and $0 < \tau < \tau_c$,

$$f_{\rm p}(c) \ \partial c / \partial x^* = R^* \quad \text{at } x^* = y^{*-}(\tau).$$
 (26)

2. Flux-limited analysis, $\tau > \tau_c$,

$$c = c_{\rm F}, \qquad x^* = y^{*-}(\tau).$$
 (27)

When $\tau = \tau_c$, both Eqs. (26) and (27) are satisfied.

• Free boundary condition

$$\frac{dy^*}{d\tau} = r^* f_{\mathbf{p}}(c) \left. \frac{\partial c}{\partial x^*} \right|_{x^* = y^{*^-}(\tau)} - \left. \frac{\partial c}{\partial x^*} \right|_{x^* = y^{*^+}(\tau)}. \tag{28}$$

• Continuity conditions at the glass-gel transition, $x^* = x_G^*(\tau)$

$$c|_{x^{*}=x_{G}^{*^{-}}(\tau)} = c|_{x^{*}=x_{G}^{*^{+}}(\tau)} = c_{G},$$

$$\left[f_{s}(c) \frac{\partial c}{\partial x^{*}}\right]_{x^{*}=x^{*-}(\tau)} = \left[f_{s}(c) \frac{\partial c}{\partial x^{*}}\right]_{x^{*}=x^{*+}(\tau)}.$$
 (29)

Equations (20) through (29) constitute a Stefan problem [6]. The methods of mathematical solution and numerical integration are described separately in a paper to be published elsewhere [7]. We define the similarity variables ξ , η by

$$\xi = x^* \tau^{-\frac{1}{2}},$$
 $\eta = \tau^{\frac{1}{2}}.$ (30)

By letting

$$y^*(\tau) = \eta \zeta(\eta),$$

$$\chi_{G}^{*}(\tau) = \eta Z_{G}(\eta), \tag{31}$$

it can be shown, for small $0 < \eta < < \eta_c = \tau_c^{\frac{1}{2}}$, the solution of the Stefan problem may be approximated [7] by

$$\zeta(\eta) \simeq \zeta_0$$
 (a constant),

$$c(\xi, \eta) \simeq c^{0}(\xi), \, \zeta_{0}^{+} < \xi < \eta^{-1},$$

$$\simeq \eta c^{1}(\xi), \, \zeta_{0}^{-} - B^{*}\eta^{-1} < \xi < \zeta_{0}^{-}.$$
 (32)

Both ζ_0 and $c^0(\xi)$ are determined from a subroutine that solves, for an arbitrary $\bar{\zeta}$, the initial value problem in the space variable ξ of the ordinary differential equation

$$\frac{d}{d\xi} \left[f_{\rm s}(\bar{c}) \bar{c} \, \frac{d\bar{c}}{d\xi} \right] + \frac{1}{2} \, \xi \, \frac{d\bar{c}}{d\xi} = 0, \qquad \bar{\zeta} < \xi < \infty, \tag{33}$$

with the initial conditions at $\xi = \bar{\zeta}$,

$$\bar{c} = c_{\rm r}$$

$$\frac{d\bar{c}}{d\xi} = -\frac{1}{2}\bar{\zeta}.\tag{34}$$

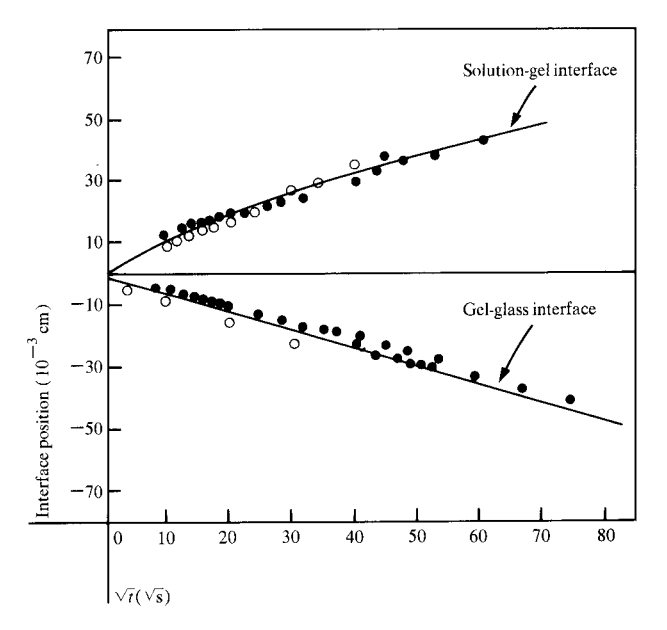


Figure 2 Positions of the gel-liquid and glass-gel interfaces plotted against the square root of the time. The open circles are calculated from the model; the solid circles are experimental values.

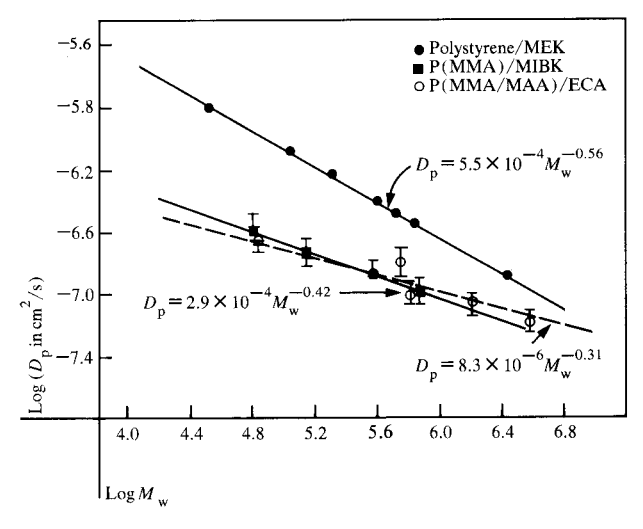


Figure 3 Diffusion coefficient $D_{\rm p}$ of some polymers in various solvents plotted against their molecular weights $M_{\rm w}$.

Among all the solutions $\bar{c}(\xi)$, we look for ζ_0 and $c^0(\xi)$ such that $c^0(\infty) \to 1$. Finally, $Z_G(\eta) \simeq Z_{G_0}$ are determined following the solution $c^0(\xi)$. The function $c^1(\xi)$ is determined from the boundary value problem of the differential equation

$$r^* \frac{d^2 c^1(\xi)}{d\xi^2} + \frac{1}{2} (\xi - \zeta_0) \frac{dc^1(\xi)}{d\xi} = \frac{1}{2} c^1(\xi),$$

$$-\infty < \xi < \zeta_0^-, \qquad (35)$$

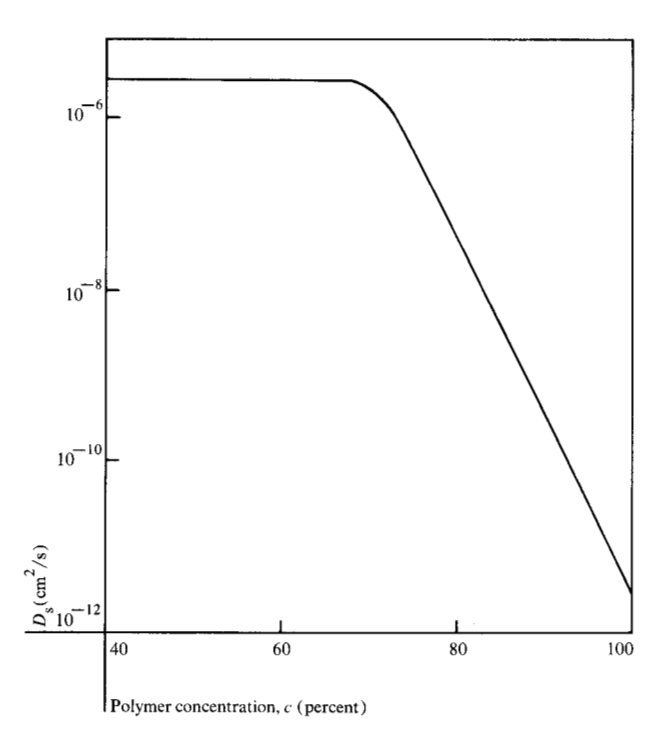


Figure 4 Diffusion coefficient $D_{\rm s}$ of MEK polystyrene against the polymer concentration.

Table 1 Material constants for the polystyrene – MEK system.

$\frac{\textit{Molecular weight}}{\textit{M}_{\text{w}} \times 10^{-5}}$	$\frac{Disassociation}{volume\ fraction}$ $\frac{c_{\rm F} \times 100}$	Disassociation rate R	
		(Å/min)	(cm/s)
0.63	70.00		
1.00	26.74	1.74×10^{9}	$2.90 \times 10^{-}$
3.00	8.91	1.22×10^{6}	$2.04 \times 10^{-}$
5.00	5.35	5.17×10^4	$8.63 \times 10^{-}$
7.00	3.82	6.64×10^{3}	$1.11 \times 10^{-}$
10.00	2.67	2.61×10^{2}	4.35×10^{-6}

subject to the boundary conditions

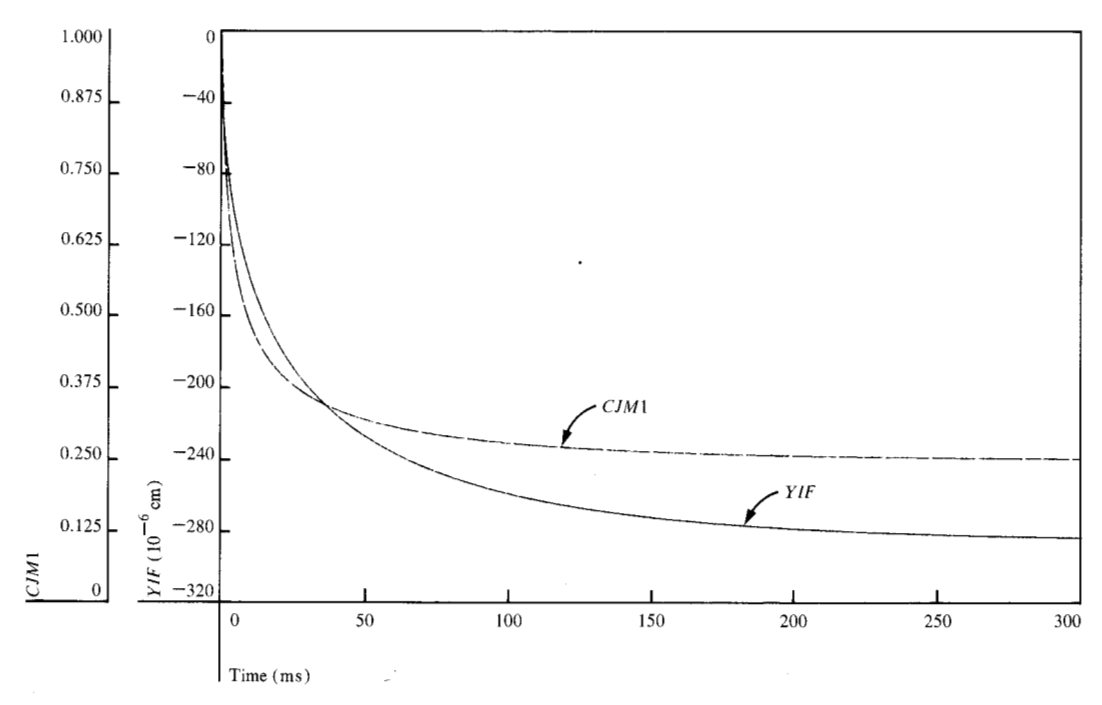
$$dc^{1}(\xi)/d\xi = r^{*}, \qquad \xi = \zeta_{0}^{-};$$

$$c^{1}(\xi) = 0, \qquad \xi \to -\infty.$$
(36)

Assuming that the initial solutions c^0 , ζ_0 , and Z_{G0} are valid for small $\tau \to 0$, we can interpret them in terms of the dimensionless space variables x^* and τ (or the physical variables x and t) by means of Eqs. (30), (18), and (19). Thus, the gel-liquid interface y(t) is given, approximately for $t \to 0$, by

$$y(t) \approx H_{\rm p} \zeta_0 \eta = \zeta_0 \sqrt{D_{\rm s}} t, \tag{37}$$

Figure 5 The polymer concentration (CJM1) at the impermeable substrate and the location of the gel-liquid interface (YIF) plotted vs time for a rubbery type polymer with the following parameters: $H_p = 10^{-4}$ cm; boundary layer thickness $B = 10^{-4}$ cm; $D_s = 3 \times 10^{-6}$ cm²/s; $D_p = 10^{-7}$ cm²/s; $C_F = 0.25$; and the disassociation rate R = 0.



and the glass-gel interface $x_G(t)$ may be computed, approximately for $t \to 0$, according to

$$X_{\rm G}(t) \approx H_{\rm p} Z_{\rm G0} \eta = Z_{\rm G0} \sqrt{D_{\rm s} t}.$$
 (38)

To continue the solution of the Stefan problem, Eqs. (20) through (29) have to be integrated numerically. The method consists of the following steps:

- 1. The moving gel-liquid interface $y^*(\tau)$ is extrapolated to the forward time level by means of an explicit forward difference expression of Eq. (28).
- 2. Equations (20) and (23) are first linearized upon the solution at τ and then replaced by the Crank-Nicholson difference operators. By this means, the concentration profiles of the forward time level can be determined algebraically.
- 3. Until the establishment of τ_c , since $\tau \le \tau_c$ when $c \le c_F$ at $x^* = y^{*-}(\tau)$, the analysis remains to be source-limited, and the boundary condition (26) is to be used. Thereafter, $\tau > \tau_c$, and the boundary condition (27) of the flux-limited analysis is to be used.

In the absence of the glass transition, no numerical complication was encountered in the calculation. However, when the glass transition does exist, we have observed that: a) there is a very sharp concentration gradient near the glass transition, and b) there is a very sharp inflection as $c \rightarrow 1$ in order to satisfy the condition

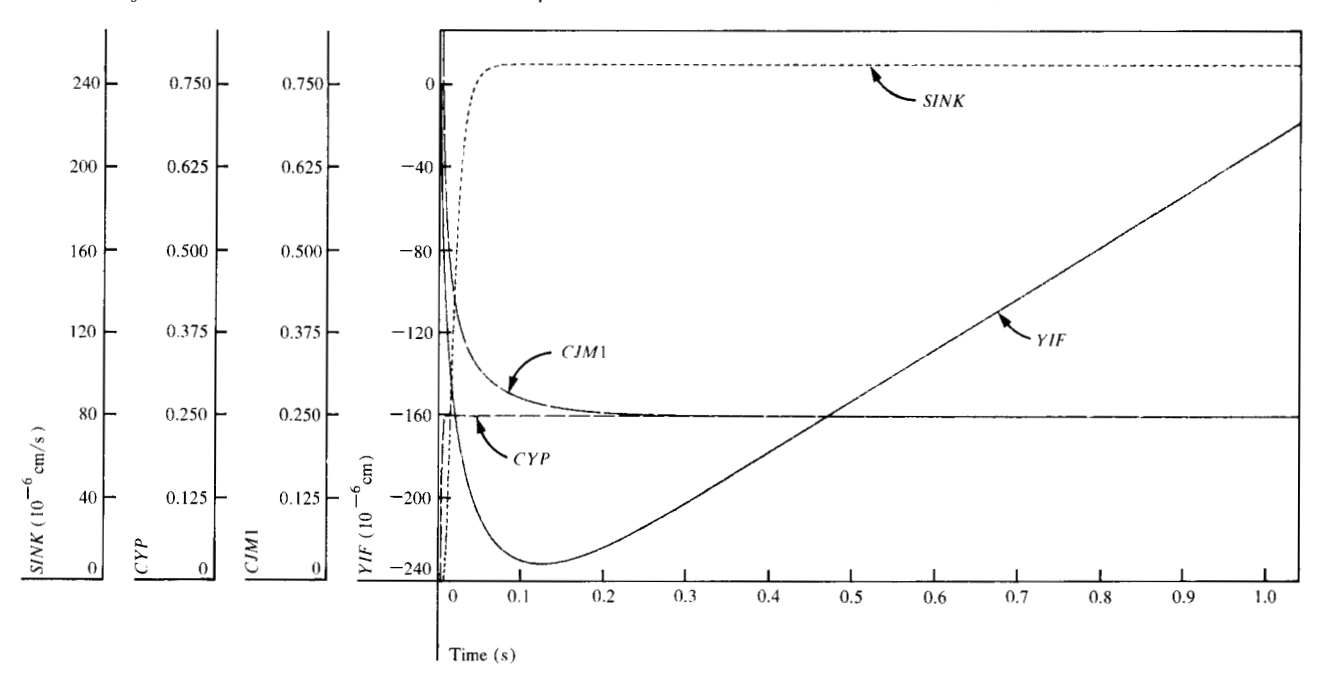
 $\partial c/\partial x^* = 0$ at $x^* = 1$ in Eq. (22). Consequently, very stringent conditions must be imposed on both the mesh size Δx^* and the time step size $\Delta \tau$ in the integration scheme. This, in fact, constitutes a very sharp boundary layer in which the exact concentration distribution is not of great interest, but for which the rate of motion is important. For this reason, and because of the extreme difficulty of carrying out a difference solution, we turned to a further approximation for the numerical solution.

To investigate the swelling and the dissolution of glassy polymer, it is therefore assumed that the concentration profile in the glassy state of the polymer may continue to be approximated by $c^0(\xi)$. In the gel layer, the concentration is so determined that the concentration is continuous at the glass-gel transition, $x^* = x_G^*(\tau)$, satisfying the first continuity condition in Eq. (29) throughout the duration of the existence of the glass phase. Thereafter, the boundary condition $\partial c/\partial x^* = 0$ at $x^* = 1$ in Eq. (22) is again used after the disappearance of the glassy phase. In view of the fact that the thickness of the gel layer, $x_G^*(\tau) - y^*(\tau)$, varies in τ , the mesh size in the gel layer is allowed to vary accordingly.

Experimental verification

Polystyrene is undoubtedly one of the most studied polymers; hence many of its physical and chemical properties that we need as input parameters to our dissolution kine-

Figure 6 The rate of removal of dissolved polymer at the boundary layer (SINK in cm/s); the liquid phase polymer concentration (CYP) at the gel-liquid interface; the polymer concentration at the impermeable surface (CJM1); and the location of the gel-liquid interface (YIF) plotted against time in the dissolution of a rubbery type polymer. The material and experimental variables are $H_p = 10^{-4}$ cm; $D_s = 3 \times 10^{-6}$ cm²/s; $R = 10^{-3}$ cm/s; and $C_F = 0.25$. The large value of R makes this example a flux-limited case.



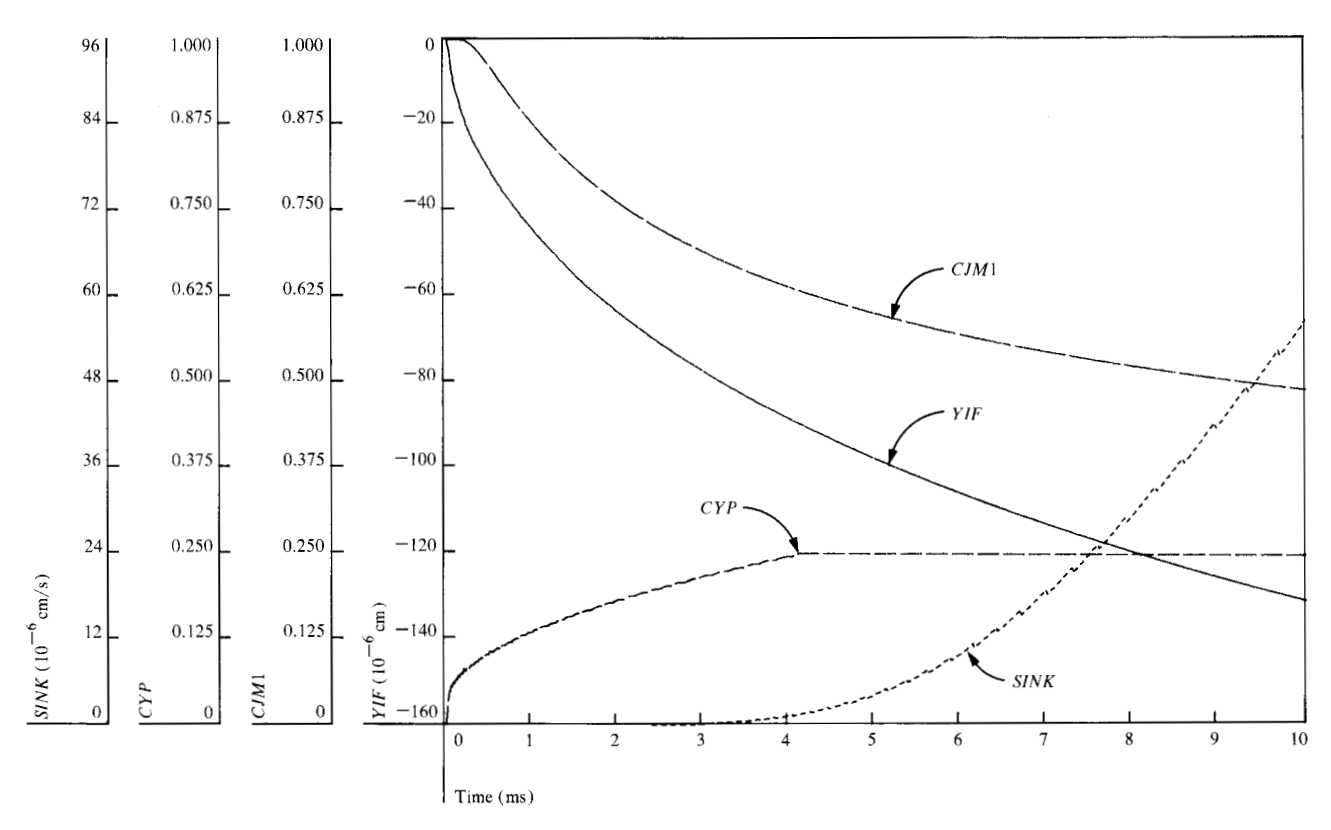


Figure 7 Expanded scale of Fig. 6. SINK, CYP, CJM1, and YIF are quantities defined in Fig. 6. The parameters are identical with those of Fig. 6.

matics model are readily available in the literature. Furthermore, Ueberreiter and his colleagues [8-10] have studied the dissolution behavior of polystyrene in many solvents. Thus, our choice of obtaining data on polystyrene dissolving in methyl ethyl ketone (MEK) to compare with our model is an obvious one.

To obtain experimental data that can be compared with computer results of the analytic model, it was necessary to develop an in situ technique for measuring the motion of the gel-glass and the liquid-gel interfaces. We succeeded in measuring the real time motion of these two boundaries by using critical-angle illumination microscopy. This technique takes advantage of the sharp change in the refractive index at the boundaries of a dissolving polymer, resulting in a marked difference in the amount of light transmitted to the objective of the microscope from the different phases (solvent, gel, glass) of the dissolving polymer. Consequently, the solvent appears dark, the gel very bright, and the glass slightly darker than the gel in the photomicrographs of NBS-705 dissolving in MEK as shown in Fig. 1. The motion of the different boundaries is measured with the aid of a fixed cross hair in the microscope and a set of micrometers that drives an x-y platen

holding the sample cell. This allows us to align the interfaces with the cross hair and thereby to follow the locations of the boundaries with time. A detailed description of the apparatus will be given in a separate paper [11].

The good agreement between the experimentally measured boundary position with time and that calculated from the model is shown in Fig. 2. It plots the positions of the liquid-gel and the gel-glass interfaces versus the square root of time for polystyrene (molecular weight 179 000) dissolving in MEK. The parameters used in the calculations of interface positions from the model corresponded closely with the physical properties of polystyrene dissolving in MEK, i.e., $D_{\rm s}=10^{-6}{\rm cm}^2/{\rm s}$, $D_{\rm p}=10^{-7}{\rm cm}^2/{\rm s}$, $c_{\rm F}=0.15$, $c_{\rm G}=0.75$, and the geometrical characteristics of the sample, $H_{\rm p}=1$ cm and B=0.5 cm.

The diffusion coefficients of polystyrene in MEK and of other polymer-solvent systems over a range of molecular weight, were obtained using Rayleigh scattering spectrophotometry [12-14]. Figure 3 shows the diffusion coefficient of polystyrene in MEK plotted against the molecular weight. In our simulation work we assumed $D_{\rm p}$ to be independent of concentration, i.e., $f_{\rm p}(c)=1$. This assumption appears to be justified by the weak de-

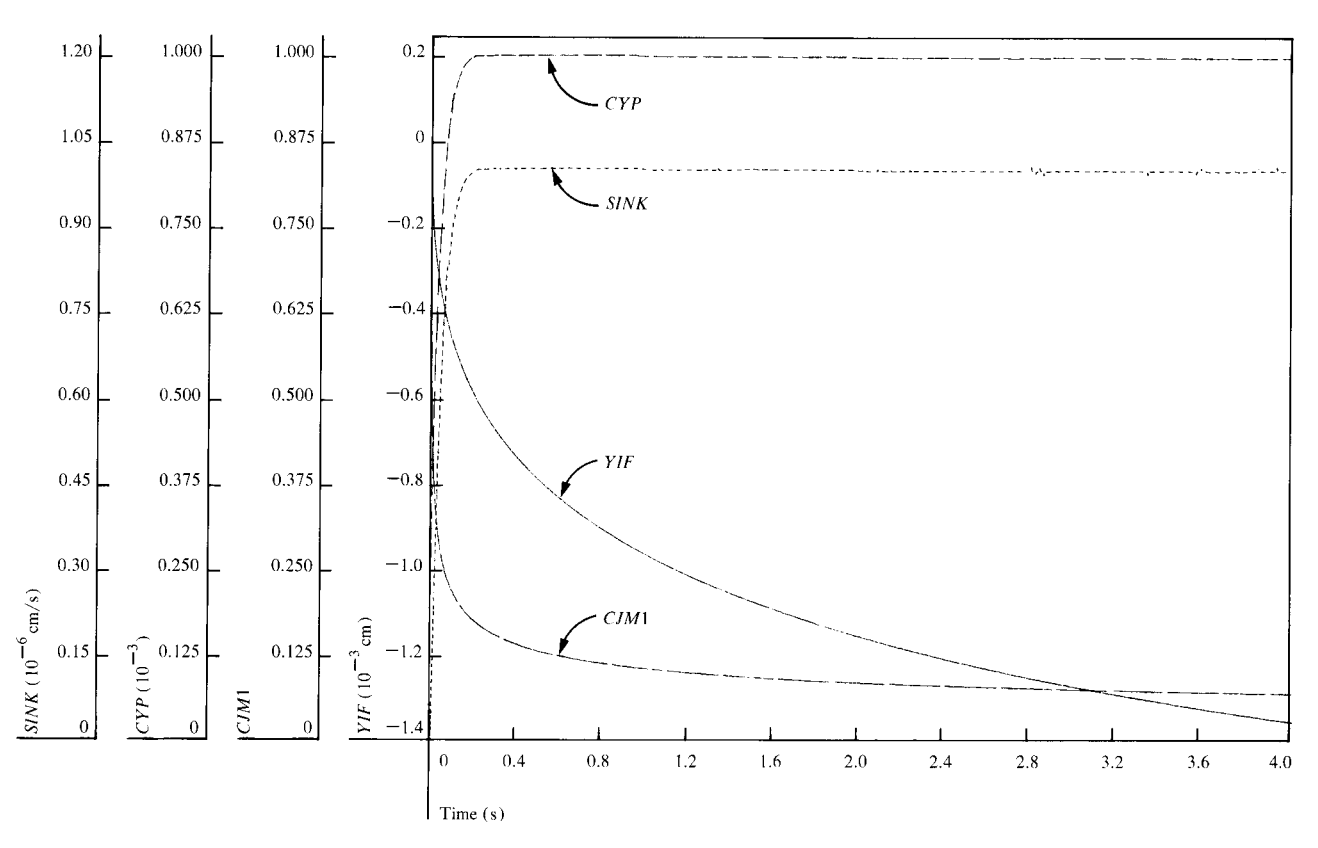


Figure 8 An example of source-limited dissolution. The flux at the boundary layer (SINK); the liquid phase polymer concentration (CYP); the polymer concentration of the impermeable surface (CJMI); and the location of the gel-liquid interface (YIF) are plotted against dissolution time in the dissolution of a rubbery type polymer. The parameters are $H_p = 10^{-4}$ cm; $B = 10^{-4}$ cm; $D_s = 3 \times 10^{-6}$ cm²/s; $D_p = 10^{-7}$ cm²/s; $R = 10^{-6}$ cm/s; and $C_p = 0.05$.

pendence of D_p on the concentration as demonstrated in the results of King, Knox, and McAdam [15].

Using Ueberreiter and Asmussen's data [2], we approximated the diffusion coefficient of solvent in polymer as a function of polymer concentration by an algebraic formula as plotted in Fig. 4. The diffusion coefficient $D_{\rm s}$ appears to be almost independent of concentration from the pure solvent to 70 percent polymer. However, from 70 to 100 percent polymer the value of $D_{\rm s}$ drops precipitously by almost six orders of magnitude. This behavior is common to many glassy polymers and the onset of a rapid decrease in $D_{\rm s}$ with polymer concentration is coincident with the transition of the swollen layer from gel-like to glass-like material.

The polymer concentration $c_{\rm F}$ at the liquid-gel boundary for the polystyrene-MEK system is obtained from the relationship $c_{\rm F} M_{\rm w} = 27\,000$ [3, 4]. Hence, for polystyrene of $M_{\rm w} = 180\,000$, the value of $c_{\rm F}$ is 0.15. The other geometrical parameters $(H_{\rm P} \, {\rm and} \, B)$ were measured from the sample and the geometrical dimensions of the dissolution cell.

In lithography, polymers are dissolved in very thin films, usually about 1 μ m thick. Consequently, it is useful to investigate the effect of the different material variables, i.e., $c_{\rm F}$, $D_{\rm s}$, etc., on the dissolution dynamics of very thin films. The following section presents examples of the simulation of polymer films 1 μ m thick.

Dissolution of polymer in the absence of glass-gel interface

In the absence of a glass-gel interface in the polymer, no sharp change in concentration gradient is expected. To investigate the effect of various physical parameters, we consider the case of constant diffusion coefficients $f_{\rm s}(c) \equiv 1$ and $f_{\rm p}(c) \equiv 1$, and use Table 1 as a guide to choose material constants. These constants are for the polystyrene-MEK system and were approximated using the Vogel relation [3]. We consider a thin polymer of film thickness $H_{\rm p}$ and boundary layer thickness $B = H_{\rm p} = 10^{-4}$ cm in all calculations, and take values for the diffusion coefficients of $D_{\rm s} = 3 \times 10^{-6}~{\rm cm}^2/{\rm s}$ and $D_{\rm p} = 10^{-7}~{\rm cm}^2/{\rm s}$.

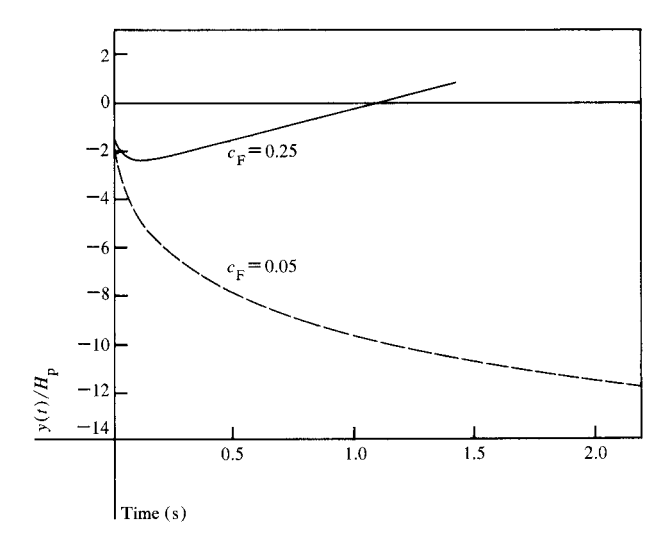


Figure 9 The effect of the gel-phase polymer concentration $c_{\rm F}$ at the gel-liquid interface on the degree of swelling of the dissolving polymer.

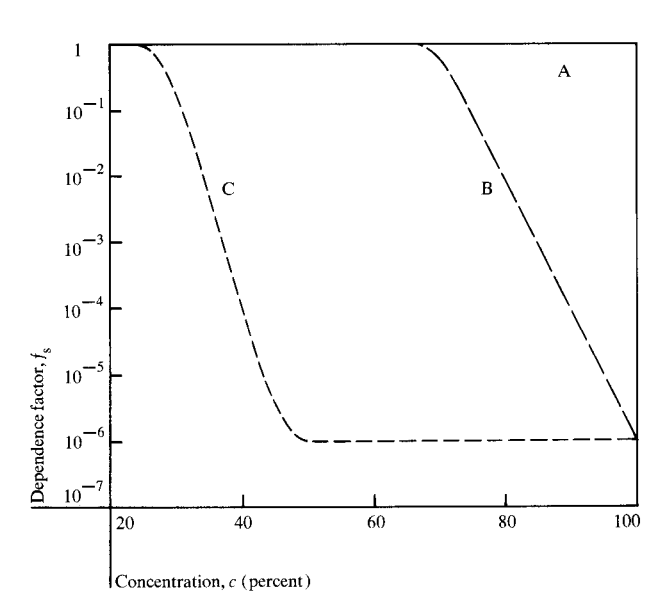


Figure 10 Concentration dependence factors of the diffusion coefficient of solvent in polymer for polymer-solvent pairs of type A, polyisobutylene in mineral oil; type B, polystyrene in MEK; and type C, polystyrene in amylacetate.

• Pure swelling, no dissolution (R=0), $c_{\rm F}=0.25$ For a non-dissolving polymer such as cross-linked systems with an equilibrium swollen polymer concentration of $c_{\rm F}=0.25$, our calculation predicts the ultimate swollen thickness of four times the original value. This has been illustrated in the computational results shown in Fig. 5. The position of the gel-liquid interface (curve YIF)

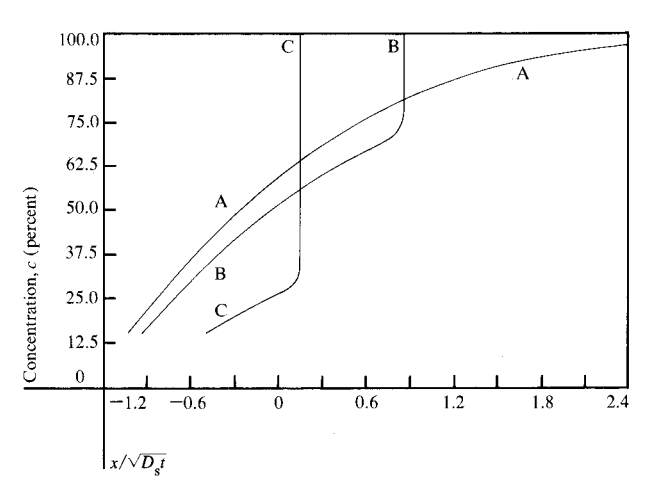


Figure 11 Similarity solutions of the concentration profile for polymer dissolution of types A, B, and C.

gradually reaches the ultimate swollen thickness as the concentration at the substrate (curve CJM) reaches $c_{\rm F}$ asymptotically.

- Dissolution of polymer of $c_{\rm F} = 0.25$, $R = 10^{-3}$ cm/s As the polymer dissolves we observe the following:
- 1. The concentration of the polymer (CYP in Figs. 6 and 7) in the liquid phase at the gel-liquid interface rises quickly and reaches $c_{\rm F}$ in about 4 ms. Figure 7 is an expanded scale of Fig. 6. Thereafter, the disassociation rate R plays no direct role in the dissolution. Hence, the dissolution is primarily diffusion-controlled.
- 2. The rate of removal (SINK in Fig. 6) of dissolved polymer at the boundary layer becomes constant in about 50 ms. The steady rate of SINK is about 25 percent of R.
- 3. The location of the gel-liquid interface (YIF) first moves in the liquid by swelling, subsequently slows down because of polymer dissolution, and then retreats after about 120 ms to complete dissolution in about 1.5 s. The maximum swollen thickness is about 2.3 times the original film thickness.
- Dissolution of polymer, $c_{\rm F} = 0.05$, $R = 10^{-6}$ cm/s The disassociation rate is quite small. We observe:
- 1. The concentration (CYP) of the liquid at the gelliquid interface rises steadily, but reaches a concentration of 0.001 (short of $c_{\rm F}=0.05$) in about 200 ms (Fig. 8). At this concentration, the flux across the boundary layer (SINK) equals the value of R (10^{-6} cm/s). Consequently, the disassociation rate R continues to control the dissolution.

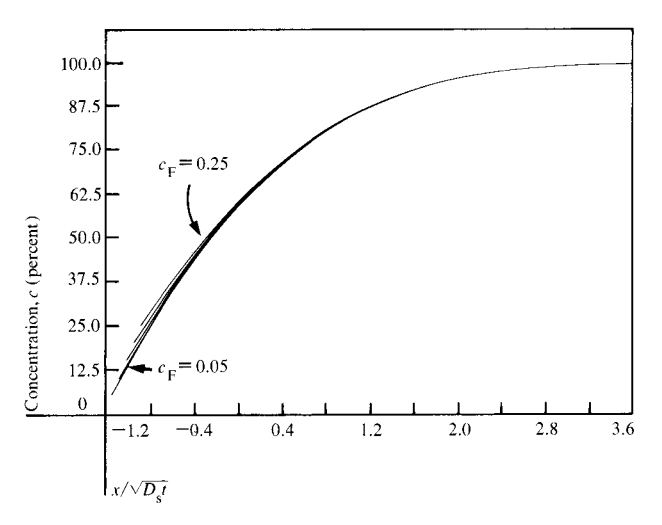
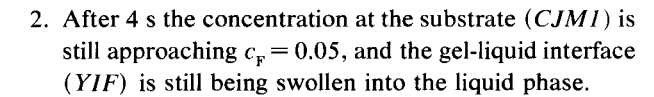


Figure 12 Similarity solutions of the concentration profile for polymer dissolution of type A with $c_{\rm F} = 0.05 - 0.25$ (in increments of 0.05).



Plotted on a common time scale, Fig. 9 shows the contrasting characteristics of the dissolution of polymers for $c_{\rm F}=0.25$ and 0.05 in the absence of glass-gel transition.

Results for initial swelling

We have investigated three types of polymer dissolution. The concentration dependence factors, $f_{\rm s}(c)$, of the diffusion coefficient of the solvent in the polymer are given by:

- 1. $f_s(c) \equiv 1$, 0 < c < 1. This is a rubbery polymer; no glassy phase exists, e.g., poly(isobutylene) in light mineral oil.
- 2. $f_s(c)$ may be approximated algebraically by

$$\begin{split} f_{\rm s}(c) &= 1, & 0 < c < 0.65; \\ &= 10^{-10\,000\,(c-0.65)^3\,(0.85-c)}, \, 0.65 < c < 0.75; \\ &= 10^{-20\,c+14}, & 0.75 < c < 1. \end{split}$$

The glass transition concentration is taken to be $c_{\rm G} = 0.75$. This type is represented by the dissolution of polystyrene in methyl ethyl ketone [2].

3. $f_s(c)$ may be approximated algebraically by

$$f_s(c) = 1,$$
 $0 < c < 0.25;$
= $10^{-96(c-0.25)^2(5-8c)}, 0.25 < c < 0.5;$
= $10^{-6},$ $0.5 < c < 1.$

The glass transition concentration is taken to be $c_{\rm G} =$

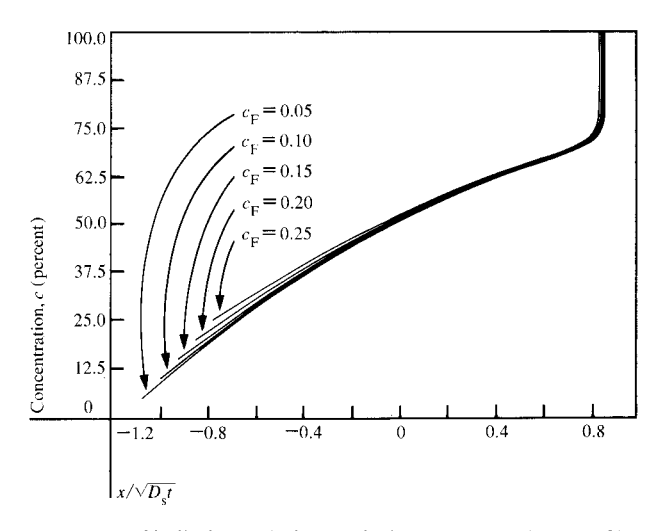


Figure 13 Similarity solutions of the concentration profile for polymer dissolution of type B with $c_{\rm F} = 0.05 - 0.25$ (in increments of 0.05).

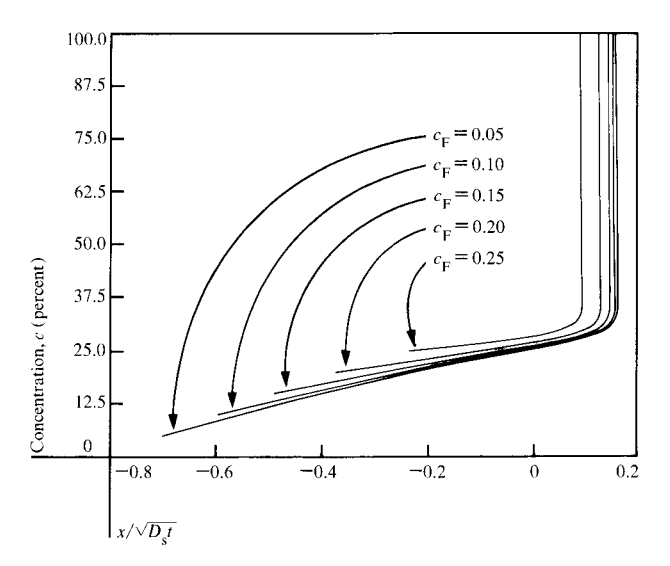


Figure 14 Similarity solutions of the concentration profile for polymer dissolution of type C with $c_{\rm F}=0.05-0.25$ (in increments of 0.05).

0.35. This type is represented by the dissolution of polystyrene in amylacetate [2].

The concentration dependence factors $f_{\rm s}(c)$ of these three types are plotted in Fig. 10 and are referred to as types A, B, and C, respectively.

The practical range of the disassociation concentration is $0 < c_F < 0.25$. The effect upon the initial swelling of these three types of polymer dissolution is shown in Fig. 11 where the initial solution $c^0(\xi)$ is plotted for $c_F = 0.15$. Figures 12, 13, and 14 show the initial solutions

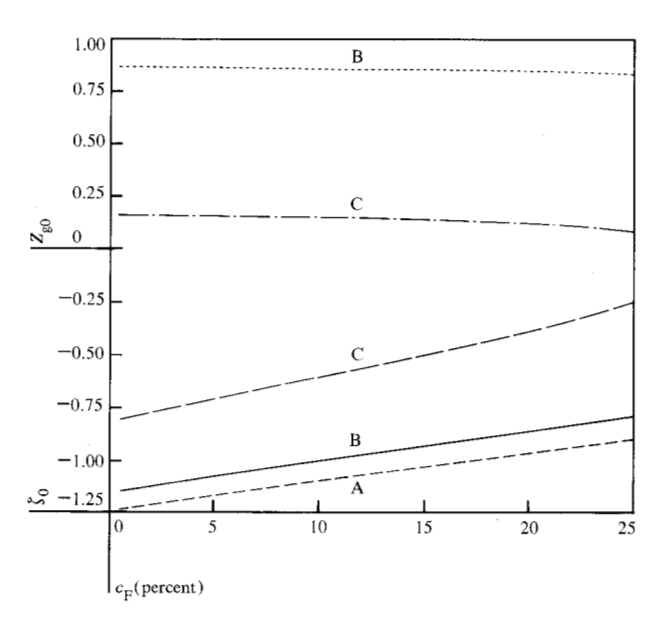


Figure 15 Initial swelling for polymer dissolution of types A, B, and C; gel-liquid interface $y(t) = \zeta_0 \sqrt{D_s} t$; glass-gel interface $x_{G0} = Z_{G0} \sqrt{D_s} t$.

 $c^0(\xi)$ for $c_{\rm F}=0.05,~(0.05),~0.25$ for types A, B, and C, respectively. The effect on initial swelling is quite pronounced for polymer dissolution of type C. The gel layer and the glassy phase of the polymer are clearly identifiable in Figs. 10, 13, and 14 for types B and C dissolution.

The gel-liquid interface y(t) and the glass-gel transition $x_G(t)$ are given by Eqs. (37) and (38), respectively, for small time t. Hence, the thickness of the gel layer in the polymer increases for small time t according to

$$x_{\rm G}(t) - y(t) \approx (\mathbf{Z}_{\rm G0} - \zeta_0) \sqrt{D_{\rm s}t}$$

The values of Z_{G0} and ζ_0 are plotted in Fig. 15.

Summary

The kinematics of polymer dissolution in one dimension can be described phenomenologically by an analytic model using material and geometrical parameters that are readily measurable. From existing data for the dissolution of polystyrene in MEK, the mathematical model is verified experimentally by an *in situ* technique measuring the motions of the glass-gel and the liquid-gel

interfaces. By means of the model we have investigated the effect of the different material parameters upon the dynamics of polymer dissolution. The simulation results show that the diffusion coefficient of solvent in polymer has a major effect on the kinematics of polymer dissolution. For example, both the rate of dissolution and the extent of swelling depend highly on the concentration dependence of the diffusion coefficient of solvent in the polymer.

References

- I. Haller, M. Hatzakis, and R. Srinivasan, IBM J. Res. Develop. 12, 251 (1968).
- 2. K. Ueberreiter and F. Asmussen, Kolloid Z. Z. Polymere 223, 6 (1968).
- G. C. Berry and T. G. Fox, Adv. Polymer Sci. 5, 261 (1968).
- 4. W. W. Graessley, Adv. Polymer Sci. 16, 1 (1974).
- 5. T. T. Wang and T. K. Kwei, Macromolecules 6, 919 (1973).
- H. G. Cohen, "Nonlinear Diffusion Problems," Stud. Appl. Math. 7, 27 (1971).
- Yih-O Tu, "A Multi-phase Stefan Problem Describing the Swelling and the Dissolution of Glassy Polymer," to be published in Q. Appl. Math.
- 8. F. Asmussen and K. Ueberreiter, J. Polymer Sci. 57, 199 (1962).
- K. Ueberreiter and W. Berrus, Ber. Bunsen. Physikal. Chemie 70, 17 (1965).
- K. Ueberreiter and P. Kirchner, Makromol. Chem. 87, 32 (1965).
- A. C. Ouano, Y. O. Tu, and J. D. Carothers, Polymer Preprint, Am. Chem. Soc. National Meeting, San Francisco, August 1976.
- R. J. Blagrove, J. Macromol. Sci. Rev. Macromol. Chem. C9(1), 71 (1973).
- Wu-Nau Huang, E. Vrancken, and J. E. Frederick, Macromolecules 6, 58 (1973).
- O. Kramer and J. E. Frederick, Macromolecules 5, 69 (1972).
- T. A. King, A. Knox, and J. McAdam, *Polymer* 14, 293 (1973).

Received April 8, 1976; revised July 29, 1976

The authors are located at the IBM Research Division laboratory, 5600 Cottle Road, San Jose, California 95193.